INTERNATIONAL JOURNAL OF PHARMACEUTICS & DRUG ANALYSIS
VOL.5 ISSUE 8, 2017; 295 – 309; http://ijpda.com; ISSN: 2348-8948

Research Article

Intermolecular change transfer in a coumarin – Aliphatic amines system: Influence of solvent and bridging unit on electronic properties

S.Bakkialakshmi*, M. Shakthi[a] & K.B. Renuka Devi[b]

**Department of Physics, Annamalai University, Annamalainagar, Tamilnadu, India-608 002.*
[a]Christ Institute of Technology, Pondicherry
[b]Rajiv Gandhi College of Engineeringand Technology, Pondicherry

Date Received: 9th July 2017; Date accepted: 21th July 2017; Date Published: 3rd August 2017

Abstract

Intermolecular electron transfer interaction between coumrin dyes (v/c) and aromatic amines, n-butyl amine (NBA) and Triethyl anine (TEA), has been investigated in three different solvents water, DMF and DMSO. The excited state intramolecular proton transfer (ESIPT) process of coumarin was fully rationalized by DFT/TDDFT calculations with optimization of the ground state (So) and exited state (S1) geometries. The molecular Electrostatic potential (MEP) map indicates the probable sites for electrophilic and nucleophilic reactive sites which interact with either solvent or quenchers (NBA and TEA). Electronic properties were derived from ground state DFT calculation. Mulliken atomic charges of coumarin with NBA and TEA in three different solvents have also been calculated.

Keywords: Coumarin, Density functional theory, Aliphatic amines, Mulliken atomic charges.

Introduction

Theoretical chemistry presents a fundamental frame work to recognize the truth on experimental observations. Computational chemistry is a branch of chemistry that utilizes the results of theoretical chemistry incorporated into efficient computer programs to calculate the structures and properties of molecules and matter, by applying these programs to real chemical problems. This important branch of science has been constructed with a strong foundation of various disciplines such as chemistry, physics, mathematics, computer science and biology. In particular, quantum chemistry demonstrates a vital role in computation chemistry which provides versatile instructions to compute electronic structure properties of molecular systems [1,2]. The Wave Function Theory (WFT) which is developed from Schrödinger equation and Density Functional Theory (DFT), which is based on Hohenberg-Kohn theorems, have achieved a remarkable level of correlation towards experimental inference [3,4].

1.1 Density Functional Theory (DFT)

Density Functional Theory (DFT) is one of the most popular approaches in quantum chemical research to solve many body electronic structure issues of molecular and condensed matter systems. This theoretical method was developed from Thomas-Fermi-Dirac model and Slater's fundamental work in quantum chemistry. This theory is identified as an essential tool to investigate various physical and chemical aspects of molecular and spectroscopic properties. The accurate description of electronic structure even for a larger system with moderate computational cost confirms the significance of DFT method [5,6,7]. DFT is completely different from traditional *ab initio* quantum chemical methods. *Ab initio* method is associated with wave-function treatment whereas DFT deals with electron density.

The net energy in terms of electron density of a system which has 'N_e' electrons can be mathematically represented as,

$$\rho_{KS}(r) = \sum \int |\Psi_i(x)|^2 \, ds \equiv \rho_{exact}(r) \quad \text{--- (1)}$$

Here, 'Ψi' represents single particle wave function. The net energy with respect to electron density functional includes following different terms namely Columbic, kinetic energy due to interaction with external potential and exchange-correlation. Therefore the function of the energy can be denoted as,

$$E[\rho] = T_s[\rho] + J[\rho] + E_{xc}[\rho] + V_{ext}[\rho] \quad \text{--- (2)}$$

Here,

$$J[\rho] = \frac{1}{2}\sum_{ij}\langle ij|ji\rangle = \frac{1}{2}\iint \rho(r_1)\rho(r_2)r_{12}^{-1}dr_1dr_2 \quad \text{--- (3)}$$

$$V_{ext}[\rho] = \int \overset{\Lambda}{V}_{ext}\,\rho(r)dr \quad \text{--- (4)}$$

In the above net energy equation, Columbic and interaction energy with respect to external potential has been defined. However, the remaining two terms such as kinetic energy ($T_s[\varrho]$) and exchange-correlation terms are not defined. In order to define these two terms, Kohn and Sham has developed certain approximations in 1965. These two theoreticians introduced an imaginary system of 'N' non-interacting electrons to be depicted by a single determinant wavefunction in 'N' orbitals 'φ_i'. The non-interacting kinetic energy of this imaginative system is precisely well known from the Kohn-Sham orbitals. This can be,

$$T_s[\rho] = -\frac{1}{2}\sum_{ij}\langle \Psi_i|\nabla^2|\Psi_i\rangle \quad \text{--- (5)}$$

The exchange-correlation function is contributed by the difference between classical and quantum mechanical electron repulsion and the variation among interacting and non-interacting system.

$$E_{xc}[\rho] = (T[\rho] - T_s[\rho]) + (V_{ee}[\rho] - V_H[\rho]) \quad \text{--- (6)}$$

Now, the Hohenberg-Kohn theorem can be implemented to yield variation in density. The single particle (Kohn-Sham) equation is

$$\left[-\frac{1}{2}\nabla^2 + V_{eff}(r)\right]\phi_i(r) = \varepsilon_i\phi_i \quad \text{--- (7)}$$

The effective potential V_{eff} (r)' with respect to electrons can be written as,

$$V_{eff}(r) = V_{ne}(r) + \int\frac{\rho(r')}{|r-r'|}dr' + V_{xc}(r) \quad \text{--- (8)}$$

Here, $V_{ne}(r)$ can be denoted by

$$V_{ne}(r) = -\sum_A \frac{Z_A}{|r-R_A|} \quad \text{--- (9)}$$

The exchange-correlation potential can be is defined as the functional derivative of exchange-correlation energy with respect to density. The mathematical representation of $V_{xc}(r)$ is,

$$V_{xc}(r) = \frac{\delta E_{xc}[\rho]}{\delta\rho(r)} \quad \text{--- (10)}$$

This Kohn-Sham equation explains the behaviour of non-interacting electrons in an effective local potential. These non-linear (Kohn-Sham) equations show the similar structure as in the Hartree-Fock equations which has non-local exchange potential (ν_x), but replaced by local exchange-correlation potential ν_{xc}. It is expressed as,

$$\left[-\frac{1}{2}\nabla^2 + \nu_{ext}(r) + \int\frac{\rho(r')}{|r-r'|}dr'\right]\phi_i(r) + \int \nu_{xc}(r,r')\phi_i(r')dr' = \varepsilon_i\phi_i(r) \quad \text{--- (11)}$$

From the equations 2 and 11, the exact ground state density and energy can be easily calculated.

1.2:Time -depended Density Functional Theory (TDDFT)

The TDDFT Kohn-Sham theory can be derived from the above said Runge-Gross theory. The orbitals generated from time-dependent Kohn-Sham equation can be given by,

$$i\frac{\partial\psi_k}{\partial t} = \left[-\frac{1}{2}\nabla^2 + V_{ext}(r,t) + V_H(r,t) + V_{xc}(r,t)\right]\psi_k(r,t) \quad \text{--- (12)}$$

This equation can be solved by explicit time-stepping strategy.

2. Materials and Methods

In the present scenario, the Onsager's model called Polarized Continuum Model (PCM) has been incorporated to study the solvent effect on molecular interactions [8].

Computational Profile

The entire quantum chemical calculations have

been performed by Gaussian09 [9] program package and the results were visualized by GassView5.0 [10] graphical user interface (GUI). The geometry optimization and ground state properties were calculated by using PBEPBE/6-31+G(d) model chemistry. The absorption spectrum was simulated from TDDFT bench using PBEPBE/6-31+G(d) model chemistry under PCM model solvated environment. The molecular interaction of Coumarin and Coumarin1 with various quenchers under different solvent system has been studied intensively. Number of solvents such as water, DMF and DMSO were incorporated individually along with different quenchers such as n-butyl amine (NBA) and tetra ethyl amine (TEA). Ground state molecular orbitals (MO's), excited state MO's and their respective band gap have been analyzed. Similarly, the experimentally observed absorption spectrum was compared with simulated adsorption spectrum along with their respective transition and oscillator strength which projects the possibility of transition.

Frontier Molecular Orbital Calculation

HOMO and LUMO are acronyms for Highest Occupied Molecular Orbital and Lowest Unoccupied Molecular Orbital, respectively. The analysis of the wave function indicates that the electron absorption corresponding to the transition from the ground state to the first excited state and is mainly described by one electron excitation from highest occupied molecular orbital to the lowest unoccupied molecular orbital.

Molecular Electrostatic Potential Analysis

Molecular Electrostatic Potential (MEP) correlates with dipole moment, electronegativity and partial charges. It provides a visual method to understand the relative polarity of the molecule. Electrostatic potential maps are very useful for three dimensional diagrams of molecules. They enable us to visualize the charge distributions of molecules and charge related properties of molecules. They also allow us to visualize the size and shape of the molecules. In organic chemistry, electrostatic potential maps are invaluable in predicting the behaviour of complex molecules.

Mulliken Atomic Charges

The quantum mechanics of Mulliken population analysis has been proposed by R. S. Mulliken [11]. This theory characterizes the electronic charge distribution in a molecule which includes the state of bonding, nonbonding and antibonding of molecular orbitals. When two normalized atomic orbitals interact together, it will produce a normalized molecular orbital. This conceptual agreement can be mathematically represented by,

$$\psi_i = c_{ij}\phi_j + c_{ik}\phi_k$$

The probability distribution of charge density can be given by

$$\psi^2{}_i = c^2{}_{ij}\phi^2{}_j + c^2{}_{ik}\phi^2{}_k + 2c_{ij}\phi_i\phi_j$$

when the atomic and molecular orbitals are normalized, then the product would be,

$$c_{ij}^2 + c_{ij}^2 + 2c_{ij}c_{ik}s_{jk} = 1$$

The overlap integral of two atomic orbital can be given by S_{jk} The C_{ij}^2 and $C_{ik}^2$are atomic orbitals population. The $2C_{ij}C_{ik}S_{jk}$ defines overlap population. If the overlap population is greater than zero then it is identified as bonding molecular orbital. If it is less than zero, then it is denoted as antibonding orbital. If the overlap population is equal to zero then it is assumed as nonbonding molecular orbital. The matrix representation of entire molecular orbitals with respect to atomic charge is called as Mulliken population matrix. The role atomic charge is crucial in the interactions between molecules.

3. Results and Discussion

On considering the computed individual molecular entities, nearly, eighteen molecular geometries were characterized via theoretical strategies such as optimized geometry, total ground state energy, frontier molecular orbital energy, vertical excitation energy, band gap, molecular electrostatic potential energy, Mulliken atomic charge, simulated UV spectral wavenumber and oscillator strength [12-17]. The treatment on Coumarin (C) with respect to quenchers such as n-butyl amine (NBA) and triethyl amine on ground of various solvents such as water, dimethyl formamide (DMF) and dimethyl sulfoxide (DMSO) exhibits about eighteen logical combinations. All the eighteen combinations were computed under polarized continuum solvation model (PCM). The visual projections and numerical data are given in this paper appropriately with

figure and table number. The theoretical interpretations were given against the computed results and plots that were projected.

Further electronic structure calculations such as ionization potential (IP), electron affinity (EA), chemical potential (μ), global hardness (η), electronegativity (χ), global softness (σ) and electrophilicity index (ω) has been calculated and tabulated in Table 1. The relationship among these quantum chemical entities can be by following mathematical relation, IP≈-E_{HOMO}, EA≈-E_{LUMO}, μ= -χ, η = (IP-EA)/2, χ = (IP+EA)/2 and ω= $\mu^2/2\eta$. In systems such as C, C-NBA, and C-TEA have their respective properties but have minor impact with respect to various solvents.

Table 1
Electronic structure properties derived from ground state DFT calculations

Systems	Electronic Structure Properties						
	IP	EA	μ	H	χ	σ	ω
C_Water	6.0080	1.8379	-3.9230	2.0851	3.9230	0.4796	16.0440
C_DMF	6.0067	1.8346	-3.9206	2.0860	3.9206	0.4794	16.0328
C_DMSO	6.0072	1.8360	-3.9216	2.0856	3.9216	0.4795	16.0370
C_NBA_Water	5.5400	1.8455	-3.6927	1.8473	3.6927	0.5413	12.5949
C_NBA_DMF	5.5329	1.8428	-3.6878	1.8451	3.6878	0.5420	12.5465
C_NBA_DMSO	5.5357	1.8439	-3.6898	1.8459	3.6898	0.5417	12.5653
C_TEA_Water	4.7228	1.8428	-3.2828	1.4400	3.2828	0.6944	7.7593
C_TEA_DMF	4.7171	1.8346	-3.2759	1.4413	3.2759	0.6938	7.7332
C_TEA_DMSO	4.7179	1.8411	-3.2795	1.4384	3.2795	0.6952	7.7352

IP- Ionization potential, EA- Electron affinity, μ - Chemical potential, χ- Electro negativity, η – Global hardness, σ – Global softness's, ω – Electrophilicity index

The PCM computation on C with respect three different solvents such as water, DMF and DMSO has been carried to report. The ground state energy, energy gap and vertical excited state energy was tabulated in Table 2, and Mulliken atomic charge was in Table 3. Graphical pictorial projections on optimized geometry, FMO's and MEP were given in Figs. 1-9. The highest ground state energy of this complex was observed in polar aprotic solvent DMF and the lowest was observed in water. Similarly, the band gap was observed high in DMF than rest of others and the vertical excitation energy is high in DMF as well. The plotted HOMO and LUMO clearly indicates the channel that allows the promotion electron from occupied to unoccupied molecular orbitals. The contributing atoms on vertical excited MO's are completely different for both HOMO and LUMO as illustrated in Figs. 1-9. The MEP map indicates the probable sites for electrophilic and nucleophilic reactive sites which interact with either solvent or quenchers. According to Mulliken atomic charge, the highest positive negative charge magnitude has been observed at C4 with 1.77261 in water solvated environment. The electron rich atom has been identified as C6 in which -0.76725 of charge. The charge hierarchy against different solvents follows the given order Water>DMSO>DMF. All the hydrogen atoms tend to have positive charge in every solvent model. And it is visualized in histogram plot of Fig. 10. The electronegativity of O10 and O11 has been exposed by intensed red surface. The μ of C all the different solvents fall on greater than -3.9 and its positive magnitude represents χ. Since the softness of the molecule is reciprocal to hardness, their values are inversely related to each other. The global electrophilicity index was greater in C against all the solvents in comparison with other different composition.

Table 2
Properties of electronic structure calculations

System	Total ground state energy	Ground State		ΔE_{GS}	Total vertical excited state energy	Vertical Excited State		ΔE_{ES}	Experimental Wavelength	Theoretical Wavelength	Oscillator strength
		HOMO	LUMO			HOMO	LUMO				
C_Water	-497.66952993	-6.00804	-1.83787	4.17017	-497.53413125	-	-	-	-	-	-
C_DMF	-497.66928636	-6.00668	-1.83460	4.17208	-497.53387135	-	-	-	-	-	-
C_DMSO	-497.66938091	-6.00721	-1.83596	4.17125	-497.53397171	-	-	-	-	-	-
C_NBA_Water	-711.17731484	-5.54000	-1.84549	3.69451	-711.04234112	-6.00859	-1.51641	4.49218	290	276	0.078
C_NBA_DMF	-711.17692097	-5.53293	-1.84276	3.69017	-711.04196774	-6.00777	-1.49925	4.50852	296	275	0.084
C_NBA_DMSO	-711.17707387	-5.53565	-1.84385	3.69180	-711.04211534	-6.41105	-1.93509	4.47596	300	277	0.083
C_TEA_Water	-789.67692005	-4.72284	-1.84276	2.88008	-789.57112124	-4.72284	-0.40283	4.32001	290	287	0.076
C_TEA_DMF	-789.67619540	-4.71713	-1.83460	2.88253	-789.57067885	-4.70542	-0.40041	4.30501	291	288	0.007
C_TEA_DMSO	-789.67671788	-4.71794	-1.84113	2.87681	-789.57104086	-4.71794	-0.41293	4.30501	292	289	0.010

Table 3
Calculated Mulliken atomic charges of Coumarin with various solvents

Atoms	Coumarin		
	Water	DMF	DMSO
C1	-0.30451	-0.30338	-0.30382
C2	-0.03851	-0.03801	-0.03820
C3	-0.48938	-0.48902	-0.48916
C4	1.77261	1.77122	1.77176
C5	-0.72849	-0.72773	-0.72802
C6	-0.76725	-0.76647	-0.76678
C7	-0.56479	-0.56513	-0.56500
C8	-0.66845	-0.66848	-0.66847
C9	0.60848	0.60731	0.60776
O10	-0.30834	-0.30774	-0.30797
O11	-0.47167	-0.46963	-0.47043
H12	0.21657	0.21611	0.21629
H13	0.21354	0.21305	0.21324
H14	0.21863	0.21800	0.21824
H15	0.22733	0.22709	0.22718
H16	0.25684	0.25631	0.25652
H17	0.26930	0.26907	0.26916
H18	0.28891	0.28842	0.28861
H19	0.26919	0.26902	0.26909

When the C interacts with quencher NBA under different solvents, a different physical behaviour was observed for each solvent respectively. The total ground state energy of the complex increased than the individual C with various solvents. The lowest energy was observed in C-NBA under water environment. The highest energy was observed in DMF solvent. But the inverse was observed with respect to band gap for the first excited state. On considering vertical excitation, the energy difference of the transition orbitals found to be 4.49218, 4.50852, 4.47596eV in water, DMF and DMSO solvent respectively. The theoretical wavelength of corresponding transition energies is 276, 275 and 277nm respectively and they are good agreement against experimentally derived absorption spectral values such as 290,296 and 300nm accordingly. On considering the oscillator strength, the values clearly indicate the possibility of achieving transitions due to appropriate wavelength in UV region. Hence, the choice of model chemistry for the TDDFT calculations appreciated. The optimized structure, FMO, transition orbitals of vertical excitation and MEP of C-NBA complex with different solvents has been given in Fig. 4-6 respectively. The Mulliken atomic charge was given Table 4.for C-NBA complex. All the optimized structures indicate the similar orientation between C and quenchers. The NBA and C were oriented one upon the other. The ground state HOMO of has been dominated by NBA moiety in water and DMSO solvent, where as it was by C in DMF solvent. But, the LUMO was often contributed by C in all the three solvent system. With respect to TDDFT transition orbitals, the HOMO of C was contributed in water and DMSO. On considering LUMO, again it was unoccupied by MO of C. This projection helps us to understand on the nature of electron transfer among occupied to unoccupied molecular orbitals. From electrostatic potential map, the highest Mulliken negative charge was observed in C20 atom and highest positive charge was observed in C4 atom. The electro-negativity of O10 and O11 was observed by red colour surface on MEP. On considering other electronic structure properties, the C-NBA show remarkable change in all the properties than in pure C under different solvent. The IP, EA, μ, η, χ, σ and ω are given as 5.5, 1.8, -3.6, 1.8, 3.6, 0.54 and 12.5 respectively.

Table 4
Calculated Mulliken atomic charges of Coumarin with NBA and TEA in various solvents

Atoms	Coumarin in NBA			Atoms	Coumarin in TEA		
	Water	DMF	DMSO		Water	DMF	DMSO
C1	-0.28236	-0.28129	-0.22212	C1	-0.22325	-0.237643	-0.22212
C2	-0.05183	-0.05069	0.04471	C2	0.04527	-0.049449	0.04471
C3	-0.65657	-0.65659	-0.48647	C3	-0.48573	-0.482266	-0.48647
C4	1.82166	1.82135	1.87988	C4	1.88149	1.858469	1.87988
C5	-0.85855	-0.85710	-1.41160	C5	-1.41313	-1.582826	-1.41160
C6	-0.60493	-0.60607	-0.47808	C6	-0.47828	-0.184974	-0.47808
C7	-0.57116	-0.57172	-0.56520	C7	-0.56543	-0.601207	-0.56520
C8	-0.62063	-0.62085	-0.59948	C8	-0.59933	-0.727909	-0.59948
C9	0.60021	0.59934	0.51667	C9	0.51678	0.699201	0.51667
O10	-0.26290	-0.26227	-0.19514	O10	-0.19567	-0.202084	-0.19514
O11	-0.45313	-0.45095	-0.43123	O11	-0.43253	-0.457917	-0.43123
H12	0.21411	0.21357	0.21523	H12	0.21552	0.216585	0.21523
H13	0.21196	0.21145	0.21234	H13	0.21263	0.213509	0.21234
H14	0.21845	0.21786	0.21718	H14	0.21755	0.217086	0.21718
H15	0.22698	0.22670	0.22316	H15	0.22329	0.224675	0.22316
H16	0.25738	0.25689	0.25728	H16	0.25756	0.256686	0.25728
H17	0.27018	0.26995	0.27031	H17	0.27055	0.270336	0.27031
H18	0.29220	0.29159	0.28961	H18	0.28988	0.289032	0.28961
H19	0.26896	0.26881	0.27217	H19	0.27226	0.269867	0.27217
C20	-0.95069	-0.94841	0.00311	N20	0.00117	-0.002694	0.00311
C21	-0.06546	-0.06679	-0.11122	C21	-0.11050	-0.128551	-0.11122
C22	-0.63654	-0.63715	0.20666	H22	0.20676	0.205906	0.20666
C23	-0.25956	-0.26002	0.21485	H23	0.21516	0.210678	0.21485
N24	-0.87482	-0.87265	-0.95832	C24	-0.95957	-0.872407	-0.95832
H25	0.22151	0.22129	0.22902	H25	0.22923	0.228965	0.22902
H26	0.22463	0.22468	0.22716	H26	0.22734	0.225707	0.22716
H27	0.22431	0.22429	0.23453	H27	0.23435	0.234359	0.23453
H28	0.22189	0.22170	-0.08538	C28	-0.08440	-0.168994	-0.08538
H29	0.22414	0.22406	0.20706	H29	0.20728	0.207943	0.20706
H30	0.21587	0.21560	0.21787	H30	0.21782	0.213229	0.21787
H31	0.22262	0.22301	-1.00655	C31	-1.00722	-1.018546	-1.00655
H32	0.21955	0.21941	0.22807	H32	0.22821	0.232067	0.22807
H33	0.20938	0.20916	0.23097	H33	0.23105	0.238718	0.23097
H34	0.39809	0.39748	0.23471	H34	0.23465	0.235864	0.23471
H35	0.38506	0.38438	-0.74059	C35	-0.73994	-0.612368	-0.74059
				H36	0.22715	0.225041	0.22702
				H37	0.22750	0.225225	0.22745
				C38	-0.48223	-0.583327	-0.48218
				H39	0.22862	0.227888	0.22819
				H40	0.22425	0.224501	0.22422
				H41	0.23388	0.241621	0.23414

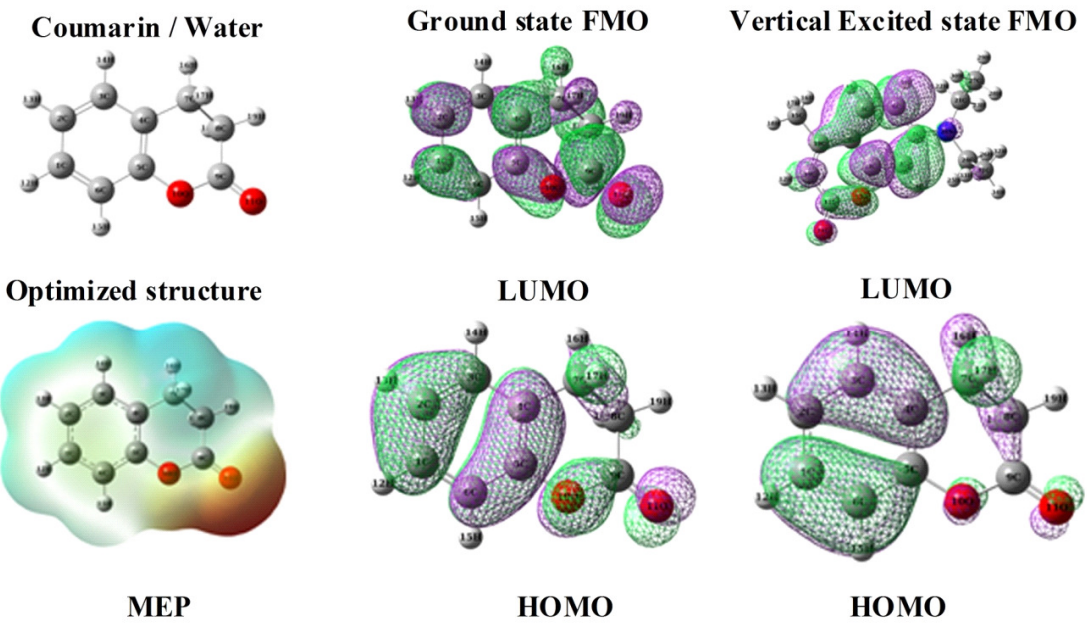

Fig.1 Optimized structure, FMO and MEP of Coumarin in water solvent

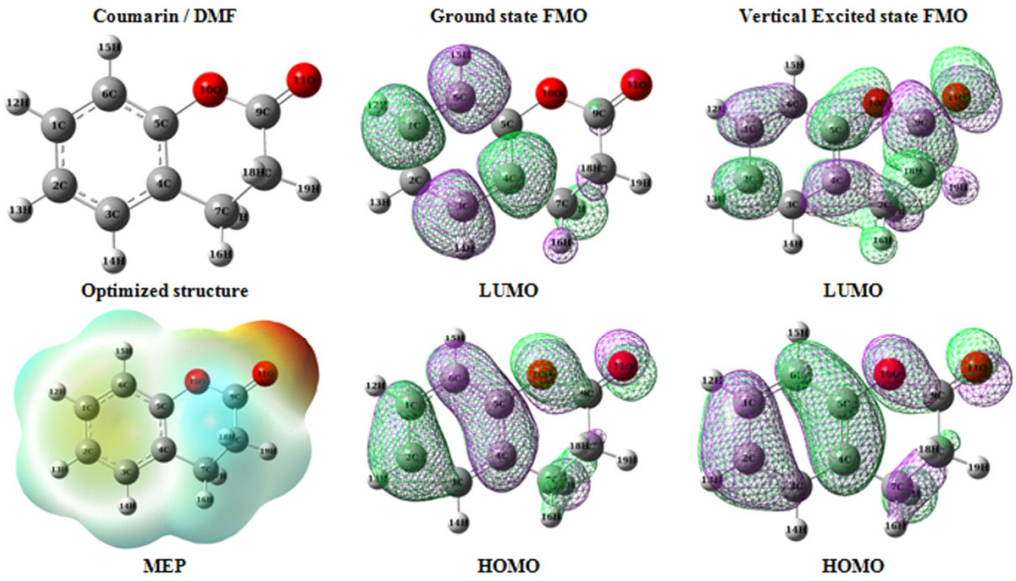

Fig.2 Optimized structure, FMO and MEP of Coumarin in DMF solvent

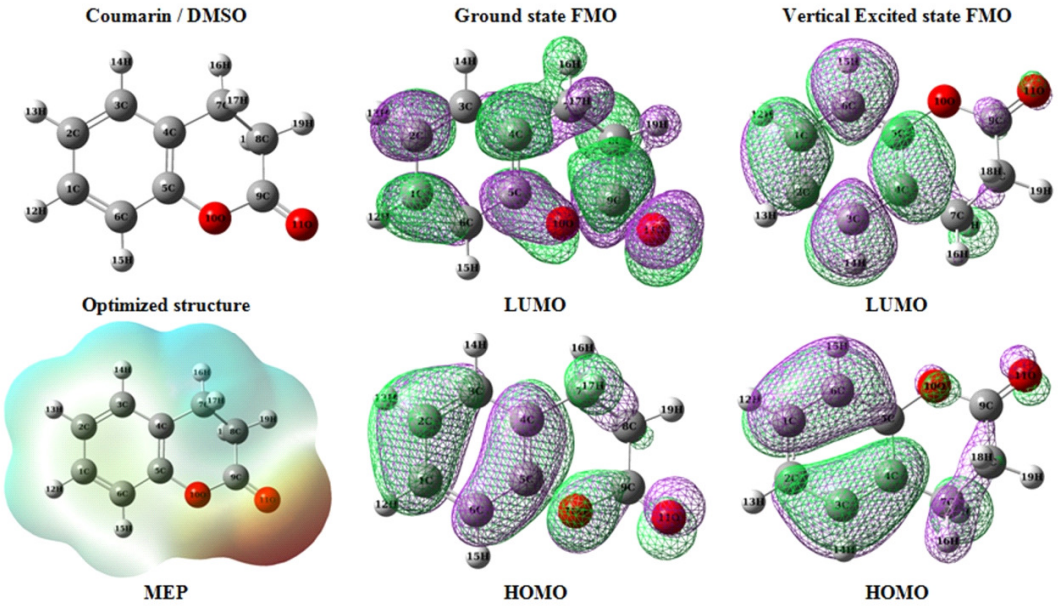

Fig.3 Optimized structure, FMO and MEP of Coumarin in DMSO solvent

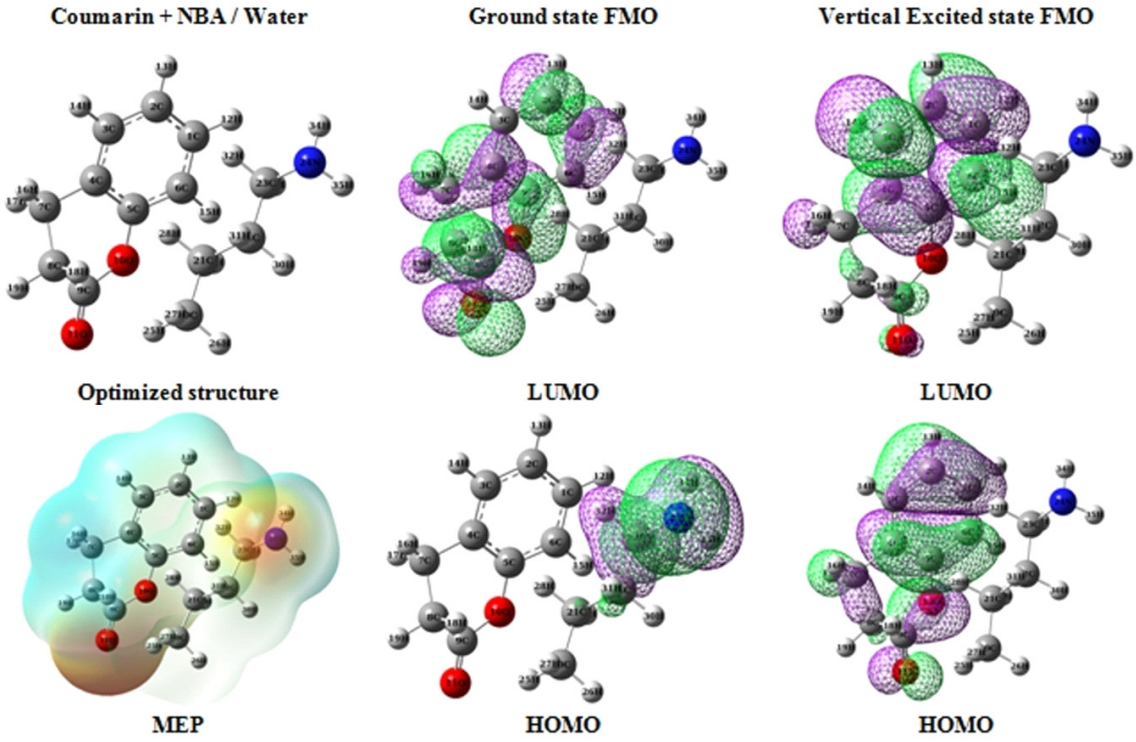

Fig.4 Optimized structure, FMO and MEP of Coumarin with NBA in water solvent

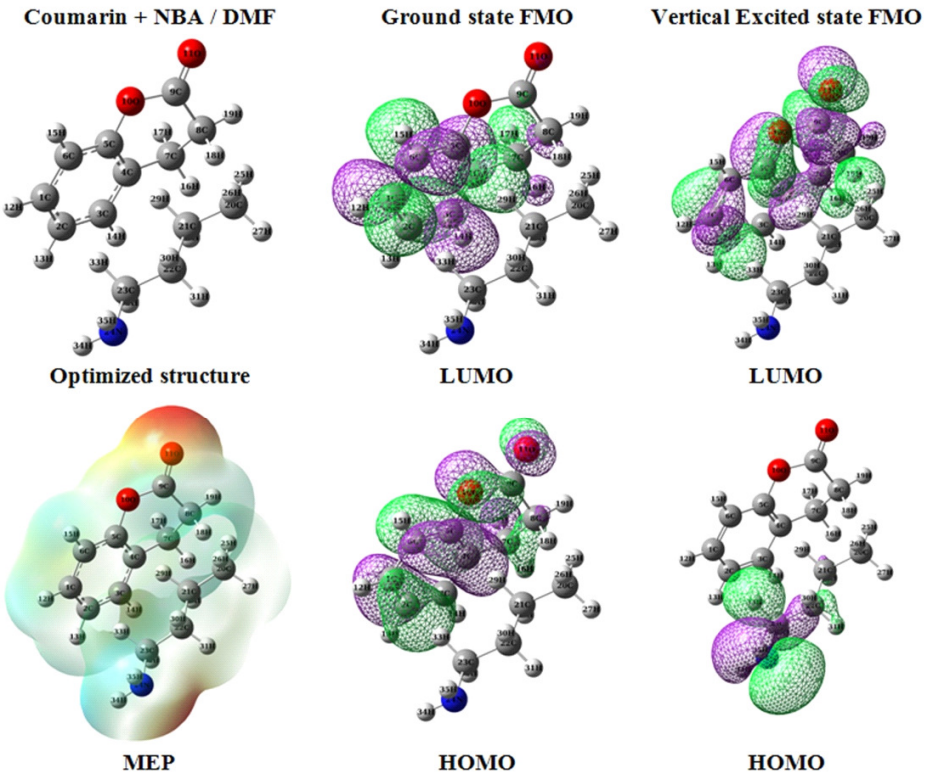

Fig.5 Optimized structure, FMO and MEP of Coumarin with NBA in DMF solvent

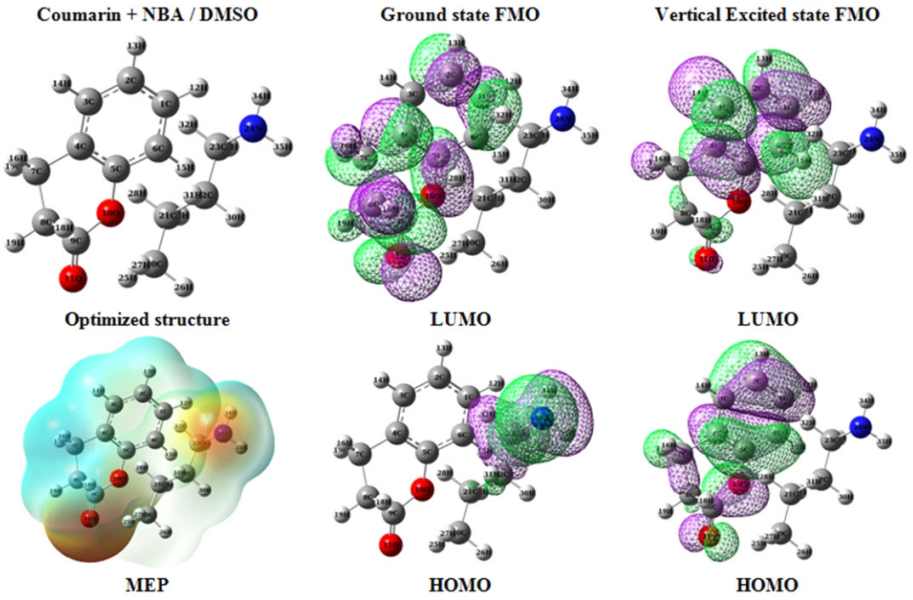

Fig.6 Optimized structure, FMO and MEP of Coumarin with NBA in DMSO solvent

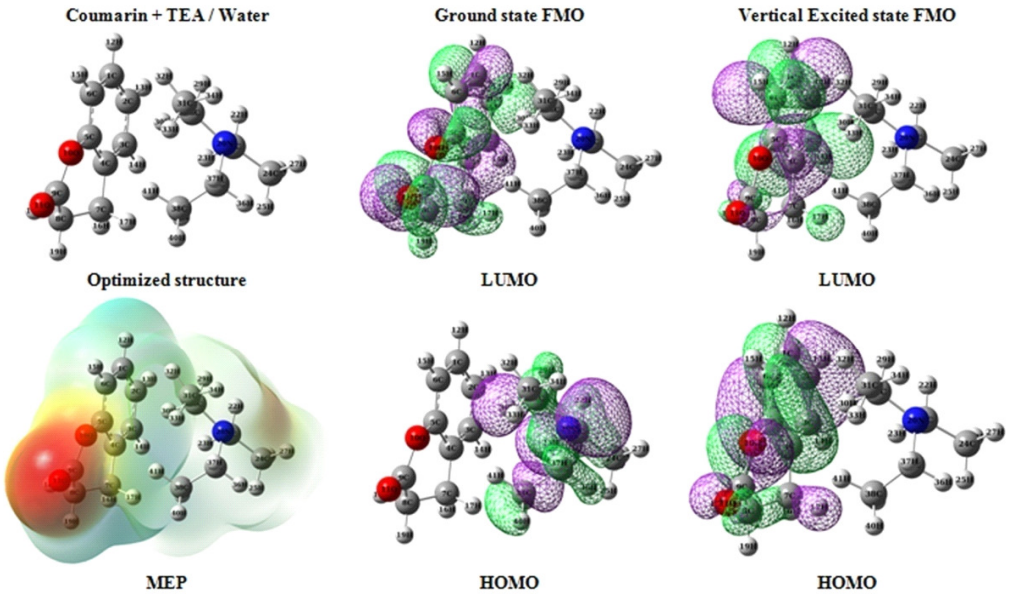

Fig.7 Optimized structure, FMO and MEP of Coumarin with TEA in water solvent

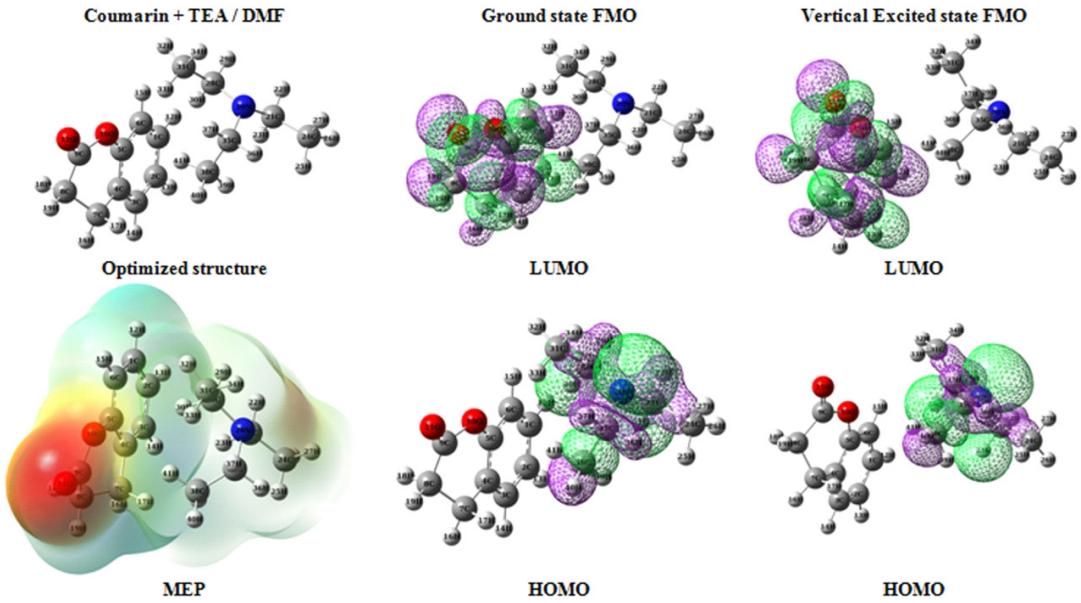

Fig.8 Optimized structure, FMO and MEP of Coumarin with TEA in DMF solvent

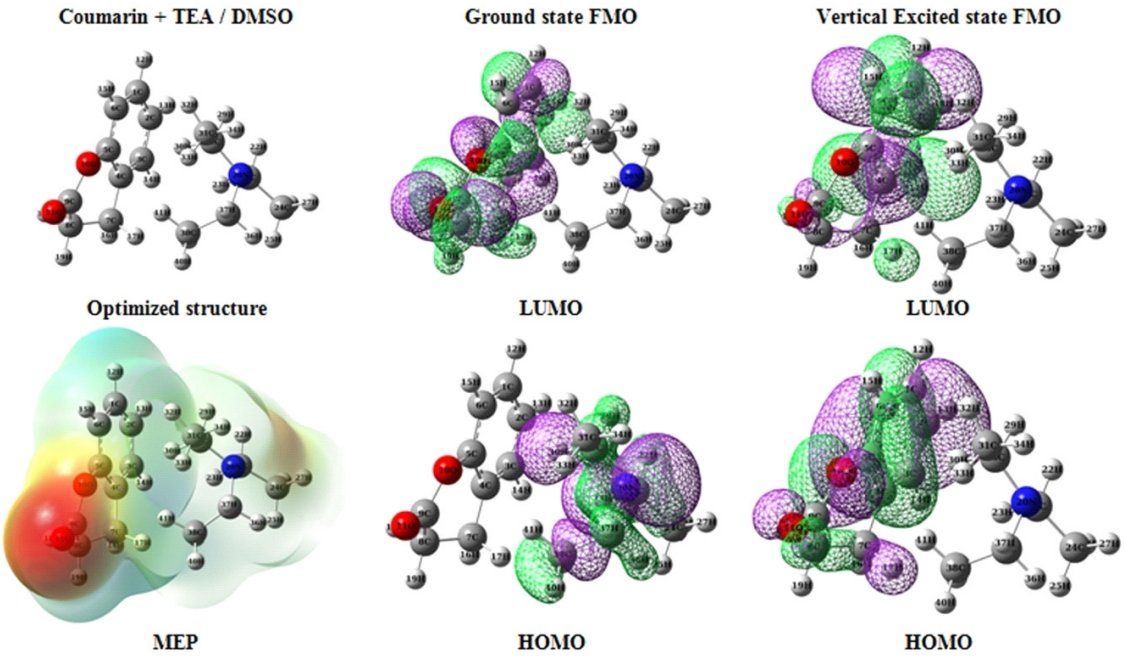

Fig.9 Optimized structure, FMO and MEP of Coumarin with TEA in DMSO solvent

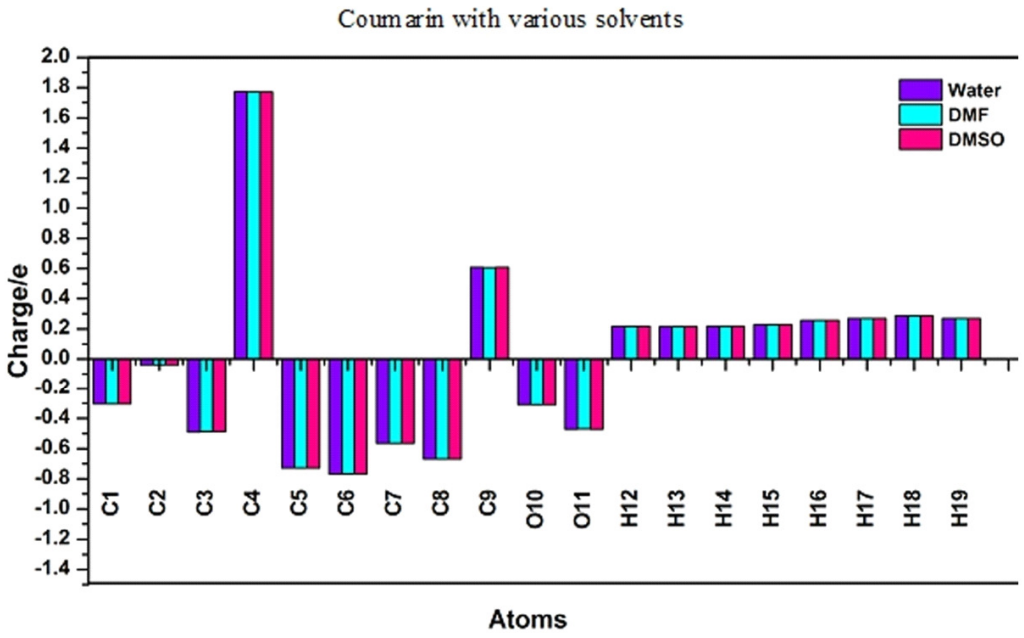

Fig. 10. Mulliken atomic charge histogram plot of Coumarin and Coumarin1 with various solvents

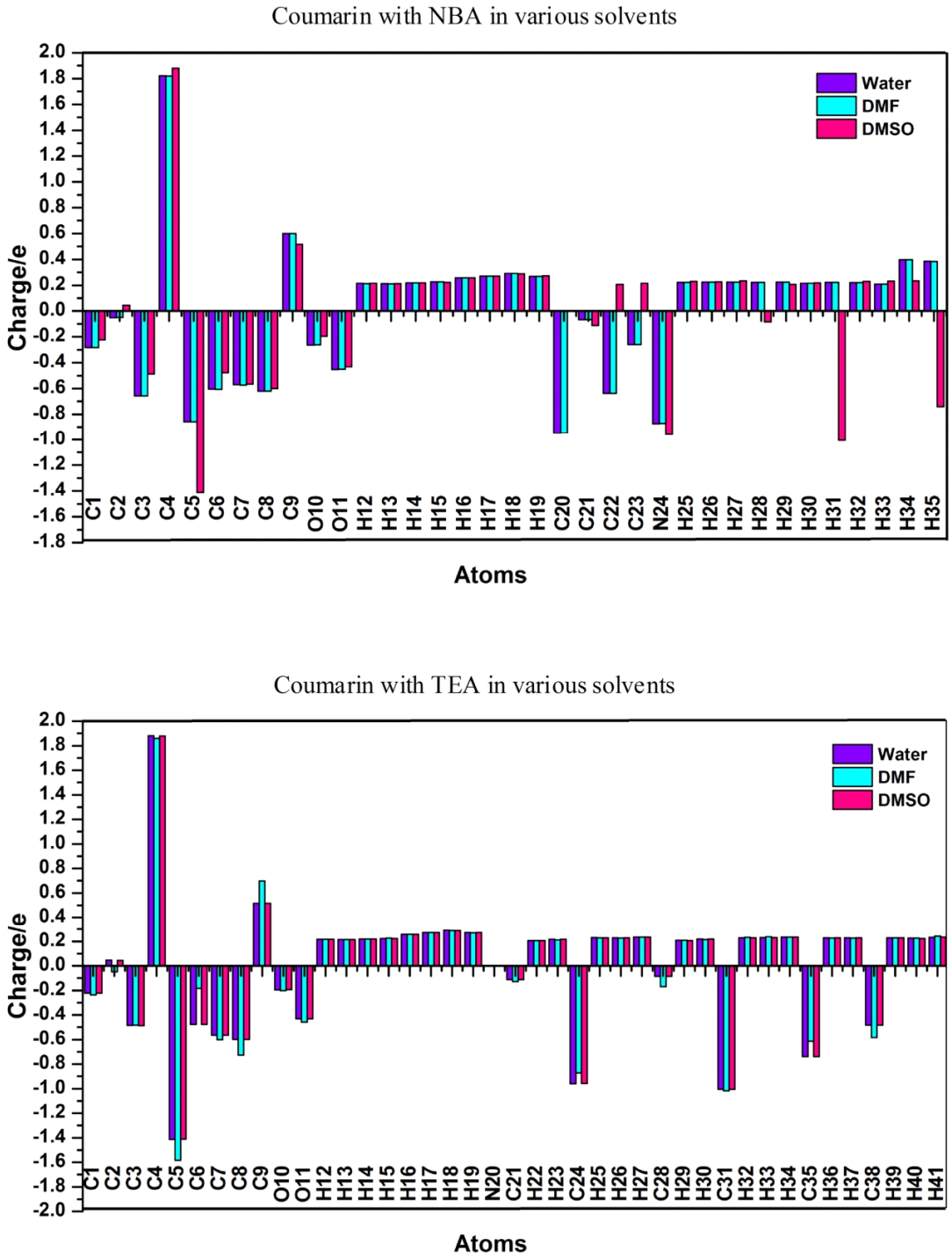

Fig. 11. Mulliken atomic charge histogram plot of Coumarin with NBA and TEA in various solvents

Alike NBA, the TEA is another quencher added to C under the same three solvent conditions. The total ground state energy of C-TEA system still reduced in comparison with quencher NBA. The higher stabilization was observed in water than the rest of the two solvents. The magnitude of band gap is not much different in the selected three solvents. Its value found to be less than 2.882eV. On experimental absorption spectrum, the observed spectrum values found to be 290, 291 and 292nm of wavelength. The simulated TDDFT spectrum has good agreement with experimental results. It was about 287, 288 and 289nm wavelength. The required energy for the transition of the respective molecular orbitals found to less than 4.32eV. The feasibility of transition has been supported by oscillator strength values namely 0.076, 0.007 and 0.10 respectively for water, DMF and DMSO solvents. The optimized structure, FMO's and MEP of C-TEA has been shown from Fig. 7-9 and the Mulliken atomic charge has been given in Table 3. The optimized orientation of C and TEA seems to be parallel to each other. On considering HOMO lobes, it was contributed from TEA moiety in all the three solvent. While on LUMO, a large involvement from C has been observed. Simulated TDDFT UV spectrum indicates the contribution from C than TEA except in HOMO of DMF solvent. These transitions of orbitals are corresponding orbitals of with respect to experimental and theoretical wavelength given in the Table 2. All the Mulliken atomic charge of hydrogen exhibits positive magnitude. However, as indicated in histogram plot in Fig. 11, the apex positive and negative charges were observed in C4 and C5 atoms. Red surface on MEP indicates the negative charge of hetero O10 and O11 atoms. With respect to other electronic structure properties such as, IP, EA, μ, η, χ, σ and ω, their values are reported in Table 1. The hardness is low and consecutively, the softness is high. Hence, C-TEA is completely sensitive against photophysical property, particularly in quenching process.

4. Conclusion

Although the calculated properties vary with respect to solvent system, a periodic trend has been observed predominately in C, C-NBA, and C-TEA, C1-NBA and C1-TEA as discussed above. The total ground state energy was notably reduced from C to C-TEA and the individuals and complexes stability increases. Similarly, the DFT calculated band gap observed as descending in nature from C to C-TEA. On comparing the ground state band gap and vertical excited state band gap, a slight higher magnitude has been observed in vertical excited state band gap. Finally, the experimentally recorded UV spectral peaks and simulated spectral peaks are in good agreement. On the whole, the theoretical and computational approach on this investigation to study the molecular interaction between Coumarin and quenchers NBA and TEA under different solvent systems has been logically rationalized to fortify the photo physical and photochemical process involved in this study.

References

[1] Schleyer, P.V.R.; Schreiner, P.R.; Allinger, N. L.; Clark, T.; Gasteiger, J.; Kollman, P, Schaefer, H.F.; *Encyclopedia of Computational Chemistry; 1st Edition,* John-Wiley, New York, **1998**.

[2] Szabo, A.; Ostlund, N.S; *Modern Quantum Chemistry Introduction to Advanced Electronic Structure Theory;* McGraw-Hill, New York, **1989**.

[3] Koch, W.; Holthausen, M. C.; A *Chemist's Guide to Density Functional Theory*; Wiley-VCH, **2001**.

[4] Jensen, F.; *Introduction to Computational Chemistry*; Wiley, **2006**.

[5] Dreizler, R. M.; Gross, E. K. V.; *Density Functional Theory; Springer*; Berlin, **1990**.

[6] Ziegler, T.; *Chem. Rev*., **1991**, 91, 651-667.

[7] Parr, R. G.; Yang, W.; *Density Functional Theory of Atoms and Molecules; Oxford University Press,* New York, **1989**.

[8] Jacopo Tomasi; Benedetta Mennucci; and Roberto Cammi; *"Quantum Mechanical Continuum Solvation Models."* Chem. Rev. **2005,** 105, 2999-3094.

[9] *Gaussian 09, Revision B.01,* M. J. Frisch, G. W. Trucks, H. B. Schlegel, G. E. Scuseria, M. A. Robb, J. R. Cheeseman, G. Scalmani, V. Barone, B. Mennucci, G. A. Petersson, H. Nakatsuji, M. Caricato, X. Li, H. P. Hratchian, A. F. Izmaylov, J. Bloino, G. Zheng, J. L. Sonnenberg, M. Hada, M. Ehara, K. Toyota, R. Fukuda, J. Hasegawa, M. Ishida, T. Nakaji-

ma, Y. Honda, O. Kitao, H. Nakai, T. Vreven, J. A. Montgomery, Jr., J. E. Peralta, F. Ogliaro, M. Bearpark, J. J. Heyd, E. Brothers, K. N. Kudin, V. N. Staroverov, T. Keith, R. Kobayashi, J. Normand, K. Raghavachari, A. Rendell, J. C. Burant, S. S. Iyengar, J. Tomasi, M. Cossi, N. Rega, J. M. Millam, M. Klene, J. E. Knox, J. B. Cross, V. Bakken, C. Adamo, J. Jaramillo, R. Gomperts, R. E. Stratmann, O. Yazyev, A. J. Austin, R. Cammi, C. Pomelli, J. W. Ochterski, R. L. Martin, K. Morokuma, V. G. Zakrzewski, G. A. Voth, P. Salvador, J. J. Dannenberg, S. Dapprich, A. D. Daniels, O. Farkas, J. B. Foresman, J. V. Ortiz, J. Cioslowski, and D. J. Fox, Gaussian, Inc., Wallingford CT, 2010.

[10] Roy Dennington, Todd Keith, John Millam, *GaussView,* Version 5, Semichem Inc., Shawnee Mission KS, **2009.**

[11] Mulliken, R. S.; **1955**, *The Journal of Chemical Physics* 23, 1833–1840.

[12] Jerzy Leszczynski, *Handbook of Computational Chemistry,* Springer, USA. **2007.**

[13] Juan Andrés.; Joan Bertrán R,; *Theoretical and Computational Chemistry: Foundations, Methods and Techniques*, Universitat Jaume, **2007.**

[14] Peter B.; John E. G.; Robert B. H.; *Molecular Modelling: Computational Chemistry Demystified*, RSC Publishing, **2012.**

[15] Thomas H.; Jan-Ole J.; Achim G.; *Computational Chemistry Workbook,* Wiley, **2009.**

[16] Jean-Marie André, *Exploring Aspects of Computational Chemistry,* Presses Universitaires de Namur **1997.**

[17] Claude Le B.; *Computational Chemistry,* Elsevier, Amsterdam, **2003.**